Earth and Planetary Science Letters 275 (2008) 138–145

Contents lists available at ScienceDirect

Earth and Planetary Science Letters

journal homepage: www.elsevier.com/locate/epsl

Hydrogen isotopes in Mariana arc melt inclusions: Implications for subduction dehydration and the deep-Earth water cycle

A.M. Shaw [a,b,*], E.H. Hauri [a], T.P. Fischer [c], D.R. Hilton [d], K.A. Kelley [a,e]

[a] Department of Terrestrial Magnetism, Carnegie Institution of Washington, Washington DC, 20015, USA
[b] Department of Geology & Geophysics, Woods Hole Oceanographic Institution, Woods Hole MA, 02543, USA
[c] Department of Earth and Planetary Sciences, University of New Mexico, Albuquerque NM, 87131-1116, USA
[d] Fluids & Volatiles Laboratory, Scripps Institution of Oceanography, UCSD, La Jolla CA, 92093-0244, USA
[e] Graduate School of Oceanography, University of Rhode Island, Narragansett, RI, 02882, USA

ARTICLE INFO

Article history:
Received 26 January 2008
Received in revised form 13 August 2008
Accepted 15 August 2008
Available online 19 September 2008

Editor: M.L. Delaney

Keywords:
hydrogen isotopes
melt inclusions
Mariana arc
subduction zones
water
dehydration

ABSTRACT

Water is carried into Earth's mantle at subduction zones via hydrous mineral phases in subducting lithospheric plates. A certain fraction of this water is released during subduction and leads to the generation of arc volcanism. The extent of lithosphere dehydration and associated hydrogen isotope fractionation are critical to understanding the global water cycle. To further understand the origin of subduction-related fluids and how water is exchanged between Earth's reservoirs, we have analyzed volatiles and δD of magmatic melt inclusions from the Mariana arc. We find high δD values, ranging from −55‰ to −12‰, indicating release of D-enriched fluids from the subducting plate into the mantle wedge. A consequence of this process is the formation of complementary hydrous mantle components that are D-enriched (mantle wedge) and D-depleted (slab). This implies that ocean island basalts (OIB) with recycled slab components should be characterized by low δD, while high δD signatures are expected from OIB containing recycled mantle wedge peridotite. These results have important implications for the hydrogen isotope evolution of terrestrial H_2O reservoirs. Based on the magnitude of subduction-related fractionations, we show that terrestrial δD variations are inconsistent with steady-state exchange of water between the mantle and surface reservoirs. We suggest that the subduction process is responsible for the present-day δD difference observed between Earth's major water reservoirs.

1. Introduction

Determining the hydrogen isotopic composition (δD) of Earth's reservoirs is important for understanding the origin of water on Earth and the extent of past and present H_2O exchange between the oceans and the Earth's mantle (δD is the permil deviation of the D/H isotope ratio from the D/H ratio of Standard Mean Ocean Water — SMOW; $\delta D_{SMOW} = 0‰$). Based on evidence for limited changes in eustatic sea level over time, and the presumed H_2O mass balance at ocean ridges and subduction zones, it has been recognized for more than a decade that exchange of H_2O between the oceans and the mantle must have been close to steady state for at least the past 600 million years (Jambon and Zimmermann, 1990; Galer, 1991; Rupke et al., 2004; Javoy, 2005). However, the present-day hydrogen isotope composition of water in the Earth's upper mantle (δD = −80 ± 10‰ (Kyser and O'Neil, 1984)) is distinct from seawater (δD = 0‰), and this difference is much larger than the hydrogen isotopic fractionation between seawater and hydrous minerals formed during alteration of oceanic lithosphere (Suzuoki and Epstein, 1976; Sakai and Tsutsumi, 1978; Lambert and Epstein, 1980; Graham et al., 1984; Vennemann and O'Neil, 1996; Saccocia et al., 2001). This observation suggests that Earth's mantle and surficial reservoirs of H_2O are not in isotopic equilibrium. Given that the oceans are a major terrestrial water reservoir and that ocean water is introduced into the mantle at subduction zones, hydrogen isotope disequilibrium between the mantle and the oceans would imply that either (1) water has not been extensively cycled into the upper mantle by subduction; or (2) additional processes act to fractionate hydrogen isotopes within the mantle–ocean H_2O cycle. Knowledge of the hydrogen isotope composition of the mantle wedge in subduction zones is thus important for estimating the efficiency of water transport through subduction zones, the degree to which H_2O is carried into the deep mantle, and the magnitude of any associated hydrogen isotope fractionations.

Insight to the nature of water in subduction zones has come from hydrogen isotope studies of volcanic fumaroles (Allard, 1983; Taran et al., 1989; Giggenbach, 1992), submarine basalts (Poreda, 1985; Stolper and Newman, 1994), and hydrous mineral phases (Deloule et al., 1991; Miyagi and Matsubaya, 2003). Each of these samples can be subject to processes that mask or shift their D/H ratios from

* Corresponding author. Postal address: MS#22 — WHOI, Woods Hole MA, 02543. Tel.: +1 508 289 3775; fax: +1 508 457 2187.
E-mail address: ashaw@whoi.edu (A.M. Shaw).

0012-821X/$ – see front matter © 2008 Elsevier B.V. All rights reserved.
doi:10.1016/j.epsl.2008.08.015

original source values. Based on measurements of fumarole gases and geothermal fluids from arc volcanoes, Taran et al. (1989) proposed that the δD values of subduction-related 'andesite' waters fall in the range of −30‰ to −10‰. However, the δD values of high-temperature fumaroles and thermal waters are often indistinguishable from local meteoric groundwater (Allard, 1983). Using combined $\delta^{18}O$ and δD systematics, Giggenbach (1992) showed that waters from geothermal and volcanic systems in circum-Pacific arcs could be described as mixtures between local meteoric waters and a common magmatic component with a δD value of −20±10‰, distinctly different from the upper mantle. However, because geothermal systems are inherently susceptible to shallow-level mixing and degassing processes, any attempts to assign an absolute δD value to underlying mantle sources are subject to uncertainties.

A more direct means of assessing subduction-related magmatic waters has come through studies of submarine basalt glasses. Poreda (1985) measured relatively high δD values (−46‰ to −32‰) in submarine glasses from the Mariana Trough and the Lau Basin, attributing these high values to a slab-derived component. By extrapolating observed values to infinite water contents, the water-rich component in these back-arc systems was assigned a δD value of −25‰ (Stolper and Newman, 1994). However, these samples do not originate from the magmatic arc, but rather from spreading centers 100–150 km behind the arc and far above the subducting lithospheric slab. Submarine basalt studies of actual arc samples are limited since most arc volcanism is either subaerial (and thus prone to severe degassing and associated δD modification (Kyser and O'Neil, 1984)), or erupted at relatively shallow ocean depths where the confining pressure is insufficient to completely retain water. Studies of hydrous minerals in subaerial arc rocks, such as amphibole, also point to a high δD source for magmatic arc water (ranging from −45 to −21‰) (Miyagi and Matsubaya, 2003). However, minerals exposed at the Earth's surface have the potential to be altered by meteoric water.

This study reports the first measurements of hydrogen isotopes in olivine-hosted melt inclusions from a subduction zone setting. Melt inclusions are samples of magma trapped within crystals which have grown in the magma prior to eruption. As a result of their enclosed environment, the volatile abundances of the melt inclusions should be less affected by eruptive degassing processes, as compared to lavas. The Mariana arc (Fig. 1) is the ideal location to study the characteristics of subducted water, because it subducts the world's oldest oceanic crust which is heavily altered by seawater (Stern et al., 2003). We show that hydrogen isotope fractionation is significant in the Marianas and, by inference, other subduction zones, and that this fractionation indicates that steady-state exchange of hydrogen isotopes between the mantle and surface reservoirs of water has not yet been reached for the Earth's deep water cycle.

2. Geologic setting and background

The Mariana volcanic arc results from the westward subduction of the Pacific Plate beneath the Philippine Plate and forms part of the 2500 km Izu–Bonin–Mariana (IBM) system (Fig. 1). Based on Ocean Drilling Program (ODP) site 801, the sediments delivered to the Mariana subduction zone consist of approximately 200 m of volcaniclastics overlain by a 100 m sequence of pelagic clay and chert of upper Cretaceous age (Stern et al., 2003). Prior studies of Mariana arc lavas (Elliott et al., 1997; Ishikawa and Tera, 1999; Newman et al., 2000; Tollstrup and Gill, 2005) and melt inclusions (Kent and Elliott, 2002) have shown that the magmas feeding the arc show varying contributions from sediment and altered oceanic crust components. Trace element ratios, ^{238}U–^{230}Th disequilibrium (Elliott et al., 1997) and B systematics (Ishikawa and Tera, 1999), suggest that the subduction component at certain volcanoes (Guguan, Pagan and Asuncion) is derived from a fluid-dominated system, presumably from altered oceanic crust. At the other end of the geochemical spectrum are

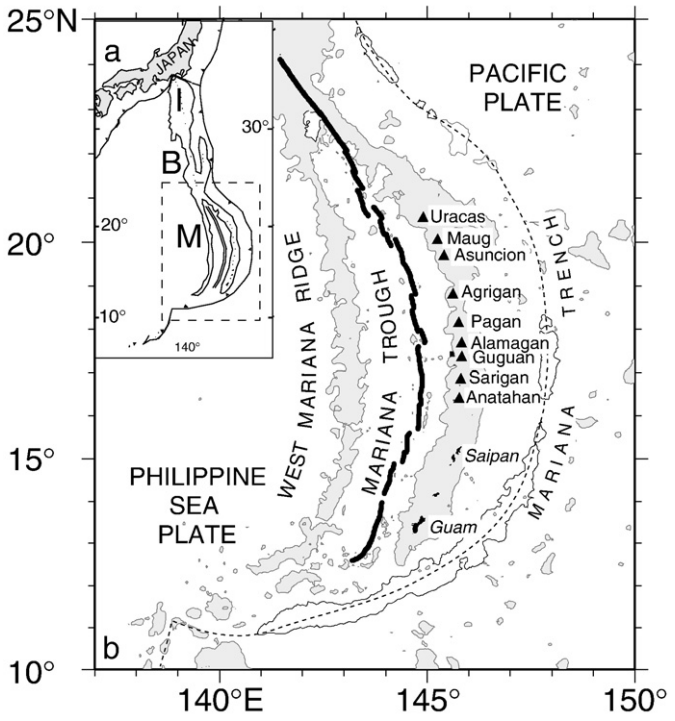

Fig. 1. a) Regional map of the Izu (I)–Bonin (B)–Mariana (M) arc system. b) Tectonic setting of the Mariana arc system — modified from Stern et al. (2003). The volcanic islands sampled in this study are identified (black triangles), along with the Mariana Trench (dashed line), and the Mariana Trough back-arc basin spreading axis and rifts. Water depths shallower than 3000 m are shown in grey.

Agrigan and Sarigan, whose geochemical signature is dominated by a sedimentary component (Elliott et al., 1997; Kent and Elliott, 2002). Determining whether these source differences are traced by H isotopes is a goal of this study.

3. Materials and methods

We have measured major elements, hydrogen isotopes and major volatile concentrations (H_2O, CO_2, F, S, and Cl) on a total of 43 naturally glassy olivine-hosted melt inclusions from 7 volcanoes along the Mariana arc, allowing for direct determination of the isotopic composition of arc-related water. All melt inclusions selected for this study were extracted from samples of air-fall scoria collected in 2003 and 2004. Major element data on the inclusions and the host olivines (Table S1 — supplementary material) were measured with a JEOL Superprobe at the Geophysical Laboratory using a 15 kV accelerating voltage, a 10 nA beam intensity and a 10 μm spot size. Hydrogen isotopes and volatile abundances were measured using the 6f Cameca ion probe at the Carnegie Institution of Washington following techniques described by Hauri (Hauri, 2002; Hauri et al., 2002). All hydrogen isotope data have been corrected for fractionations associated with matrix effects (known to vary with host compositions) and instrument mass fractionation encountered during analyses — see Hauri et al. (2006).

3.1. Correction of melt inclusion compositions

Melt inclusion data reported in Table 1 have been corrected for post-entrapment formation of a shrinkage bubble (when present), which is caused by differential contraction of melt and host crystal during cooling. This was done by measuring the size of the melt inclusion and the vapor bubble (using a scanning electron microscope — SEM), and calculating their volumes using the equations

Table 1
Major element, volatile and hydrogen isotope data from Mariana melt inclusions

Volcano	Sample ID[a]	SiO_2[b] (wt.%)	TiO_2 (wt.%)	Al_2O_3 (wt.%)	FeO (wt.%)	Fe_2O_3 (wt.%)	MnO (wt.%)	MgO (wt.%)	CaO (wt.%)	Na_2O (wt.%)	K_2O (wt.%)	P_2O_5 (wt.%)	H_2O (wt.%)	CO_2 (ppm)	F (ppm)	S (ppm)	Cl (ppm)	% olivine added	δD (‰)	Error[c] (‰)	Psat (bars)
Asuncion	ASUN-20-2_1	53.6	0.76	16.93	8.80	0.86	0.15	4.65	8.96	2.51	0.63	0.10	1.78	92	452	1050	1287	3.9	−49	2.7	518
	ASUN-20-2_3B	49.7	0.80	16.89	9.39	0.92	0.18	5.44	10.97	2.07	0.41	0.10	2.87	28	176	1561	776	4.1	−28	2.2	871
	ASUN-20-2_5	47.0	0.87	18.33	9.76	0.97	0.19	5.98	12.73	2.41	0.39	0.09	1.01	262	231	1662	884	4.4	−53	1.9	658
	ASUN-20-2_6*	47.0	0.84	17.50	10.62	1.08	0.23	6.10	11.08	2.15	0.38	0.09	2.64	165	242	1761	920	3.2	−31	1.5	1048
	ASUN-20-01_2	47.4	0.62	18.51	7.94	0.81	0.16	6.08	11.91	1.43	0.39	0.10	4.31	516	245	1671	968	3.0	−38	1.9	2768
	ASUN-20-01_11*	53.3	0.79	16.17	8.66	0.90	0.17	4.46	9.42	1.35	0.59	0.08	3.80	321	331	1119	1314	1.9	−45	2.0	2043
	ASUN-20-01_13*	53.0	0.80	16.65	8.26	0.88	0.17	4.67	9.10	1.29	0.56	0.11	4.21	345	322	1201	1291	1.1	−45	2.1	2358
	ASUN-20-01_15	51.3	0.68	17.44	7.76	0.81	0.17	5.35	10.09	1.36	0.49	0.08	4.16	782	288	1364	1123	1.8	−49	1.8	3176
Agrigan	AGRI2-27	49.8	1.00	16.34	7.55	0.79	0.21	5.32	10.58	2.61	0.78	0.25	4.46	4	464	1232	962	1.7	−19	3.0	1794
	AGRI2-31	48.1	0.89	16.19	10.04	0.92	0.20	5.54	11.21	2.48	0.64	0.16	3.43	5	432	1030	826	6.1	−51	3.1	1134
	AGRI2-32	47.9	0.83	16.24	10.02	1.01	0.19	5.10	11.35	2.25	0.59	0.20	4.06	5	465	1432	865	3.1	−49	2.8	1528
	AGRI2-38B	48.3	0.90	16.77	9.34	0.97	0.21	5.00	11.56	2.38	0.60	0.13	3.59	6	414	1083	832	2.0	−39	2.6	1232
	AGRI2-42	45.7	0.68	17.44	8.83	0.92	0.18	6.43	12.27	1.94	0.43	0.09	4.81	113	319	1519	696	2.2	−30	2.3	2285
	AGRI2-43	45.7	0.63	17.62	8.61	0.88	0.21	6.44	12.18	1.85	0.42	0.09	5.05	178	300	1581	710	2.8	−23	2.4	2590
	AGRI2-54	45.6	0.61	17.69	8.85	0.89	0.22	5.81	12.44	2.01	0.44	0.13	5.06	50	257	1510	717	3.1	−38	2.0	2327
Pagan	PAGAN5-2_1	47.3	0.60	16.13	10.03	1.09	0.24	6.86	12.34	1.95	0.43	0.06	2.85	30	264	811	553	0.7	−21	2.2	860
	PAGAN5-2_5	52.1	1.26	15.07	10.27	1.14	0.24	4.14	8.79	3.24	1.07	0.29	2.23	194	405	360	1042	−0.5	−19	2.0	920
	PAGAN5-2_15	50.1	0.92	14.83	10.50	1.08	0.19	6.58	10.25	2.61	0.82	0.11	1.94	60	253	323	439	3.4	−12	3.3	508
	PAGAN5-2_18	52.3	1.44	14.65	9.56	1.03	0.22	5.31	9.26	3.04	1.20	0.25	1.57	60	292	95	973	0.8	−49	3.3	379
	PAGAN5-2_24	52.0	1.17	14.77	10.32	1.09	0.23	5.57	9.22	2.91	1.04	0.18	1.37	169	355	399	766	1.8	−31	3.3	551
	PAGAN5-2_78	48.4	0.74	15.78	10.18	1.06	0.23	6.58	11.38	2.55	0.57	0.08	2.27	57	205	949	498	2.4	−36	3.6	641
Alamagan	ALA-02_1	47.2	0.57	15.93	7.90	0.83	0.13	7.82	13.52	1.42	0.44	0.09	3.81	169	270	1535	1072	2.0	−12	2.3	1727
	ALA-02_5*	46.7	0.59	17.57	8.03	0.88	0.17	6.96	11.98	1.32	0.59	0.09	4.65	1384	247	1755	971	0.0	−28	2.3	4531
	ALA-02_6*	47.3	0.58	17.08	8.12	0.85	0.18	7.37	12.41	1.26	0.34	0.04	4.17	750	218	1464	888	2.1	−19	2.1	3125
	ALA-02_7	55.8	1.01	15.09	9.36	1.12	0.23	3.73	7.52	1.67	1.23	0.15	2.82	174	479	772	1284	−3.2	−36	1.9	1162
	ALA-03_9	46.4	0.63	18.48	7.49	0.66	0.13	6.42	13.98	1.54	0.46	0.09	3.37	181	324	1998	1022	7.5	−39	2.1	1482
	ALA-03_16	55.7	0.90	16.83	5.97	0.67	0.14	4.27	8.78	2.03	1.52	0.17	2.71	124	687	511	1730	−0.9	−51	2.0	993
Guguan	GUG-3_11	52.2	1.16	14.66	11.74	1.33	0.28	4.56	7.91	2.89	0.53	0.12	2.45	92	342	324	1001	−1.4	−47	3.0	798
	GUG-3_16	52.4	1.02	15.67	10.46	1.23	0.23	4.12	8.46	3.00	0.59	0.10	2.58	30	328	353	1111	−2.6	−30	3.0	725
	GUG-3_38	51.5	1.02	16.99	8.10	0.95	0.22	4.70	9.76	3.01	0.57	0.13	2.86	33	293	601	1012	−2.7	−19	3.8	874
	GUG-3_41	50.3	1.04	16.32	10.02	1.16	0.22	4.63	9.46	2.62	0.57	0.12	3.37	54	304	809	973	−2.2	−31	2.9	1208
	GUG-3_44*	47.7	0.75	16.74	9.98	1.09	0.21	5.58	11.59	1.86	0.33	0.04	3.91	125	277	1029	747	0.1	−13	2.9	1698
Sarigan	SARI-15-02_2*	47.6	0.57	14.91	8.26	0.86	0.16	8.27	13.45	1.50	0.24	0.06	3.84	326	170	1667	531	3.0	−49	2.1	2077
	SARI-15-02_10	47.2	0.57	14.87	8.45	0.84	0.16	8.79	13.45	1.40	0.27	0.05	3.68	262	172	1818	570	5.1	−34	2.0	1847
	SARI-15-02_19*	47.3	0.59	15.17	8.56	0.85	0.15	8.68	13.44	1.32	0.27	0.06	3.32	340	154	1652	485	5.0	−20	2.3	1789
	SARI-15-03_1	47.9	0.57	15.20	8.54	0.90	0.19	7.83	13.09	1.42	0.41	0.08	3.58	236	201	2070	735	1.9	−23	1.9	1727
	SARI-15-03_3	47.8	0.71	16.33	8.40	0.70	0.13	7.46	12.98	1.07	0.23	0.06	3.84	151	201	1690	559	10.0	−33	1.9	1708
	SARI-15-03_6	47.9	0.67	15.87	8.81	0.92	0.18	7.49	12.55	1.49	0.34	0.06	3.45	143	202	1739	601	2.6	−51	1.9	1448
Anatahan	ANAT04rh_92*	52.9	0.90	13.58	13.43	1.65	0.38	4.85	7.03	2.08	0.90	0.22	1.77	156	493	1129	1179	−5.8	−32	2.5	654
	ANAT04rh_94	54.3	0.81	14.49	11.09	1.57	0.34	4.06	6.70	2.58	1.04	0.18	2.59	51	491	1141	1269	−13.0	−32	2.8	775
	ANAT-04_42	55.9	0.94	15.14	9.48	1.02	0.22	3.38	7.24	3.07	1.15	0.20	2.00	127	515	1087	1117	0.6	−55	2.8	678
	ANAT-04_43	55.5	0.96	15.29	9.74	1.03	0.23	3.50	7.33	3.16	1.21	0.19	1.64	52	496	804	1028	1.3	−50	3.2	383
	ANAT-04_44	55.7	0.90	15.31	9.00	1.02	0.23	3.26	7.04	2.83	1.11	0.24	3.12	117	537	1138	1163	−0.9	−21	3.3	1198

Analytical uncertainties are ±3% for major elements (±15% for P_2O_5) and ±10% for volatiles.
[a] Melt inclusions identified with an asterisk contained a vapor bubble (due to shrinkage during cooling) and have been corrected following procedures outlined in text — uncorrected values are included in Table S2 in the Appendix.
[b] All data has been corrected for host olivine interaction assuming a Fe^{3+} fraction of 0.11.
[c] Errors represent analytical uncertainties reported at the 1 sigma level.

for the volume of a sphere (bubble) and volume of an ellipsoid (inclusion). We then calculated the number of moles of gas present in the bubble with the ideal gas equation ($n = PV/RT$). We used the vapor saturation pressure derived from CO_2 and H_2O contents measured in the glass inclusions by SIMS (solubility model of Dixon and Stolper, 1995), and a glass transition temperature of 700 °C. Mole fractions of CO_2 and H_2O in the vapor were calculated, and the calculated vapor was then added back to the mass of the inclusion. This "bubble correction" typically increased the inclusion H_2O content by <2%, as compared to CO_2 contents which were increased by as much as 80%. Because the change in the H_2O content is minor, the maximum associated change in the δD of the inclusion is <0.5‰. Uncorrected melt inclusion compositions, inclusion size and bubble diameter are reported in Table S2 (Supplementary material).

An additional correction was made to account for post-entrapment crystallization of host olivine inside the inclusion, assuming a Fe–Mg K_D [=$(FeO/MgO)_{olivine}/(FeO/MgO)_{melt\ inclusion}$] of 0.3 and that 0.11 of the total FeO is Fe^{3+} (Walker et al., 2003).

4. Results

Corrected volatile, major element and H isotope data are reported in Table 1. δD values of Mariana arc melt inclusions range from −55‰ to −12‰ (Fig. 2), significantly higher than upper mantle MORB values (−80±10‰) and encompassing the range proposed for the non-meteoric component of arc fumaroles (−20±10‰). In order to evaluate the significance of these results, we must first consider processes that may have modified their original H isotope compositions. Various shallow-level, post-entrapment processes have the potential to modify the hydrogen isotope composition of magma trapped in melt inclusions.

4.1. Post-entrapment diffusional hydrogen loss

Diffusive loss of hydrogen can result in elevated δD values in slowly-cooled melt inclusions (Hauri, 2002). Several lines of evidence indicate that our inclusions have not suffered significant hydrogen

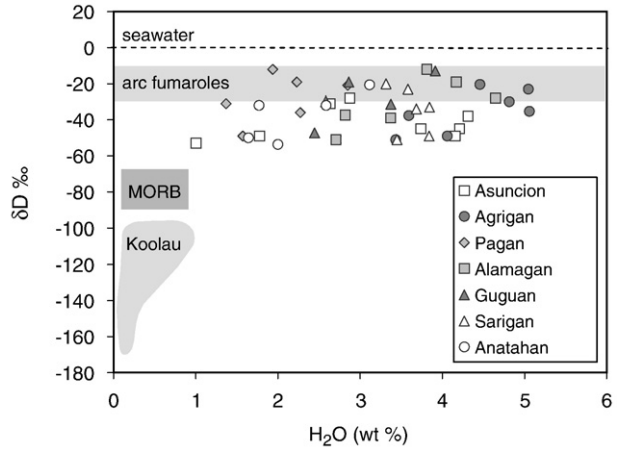

Fig. 2. δD variations as a function of water content in Mariana arc melt inclusions. Errors are smaller than the size of symbols. The shaded boxes show the range proposed for arc fluids based on fumaroles (Giggenbach, 1992), as well as the MORB range. The dashed line indicates modern seawater at 0‰. The Koolau melt inclusion field (Hauri, 2002) is included for comparison. Note that Mariana arc melt inclusions have significantly higher water contents and δD values than MORB samples.

loss. First, the absence of quench crystals in our inclusions, and the glassy nature of the scoria samples, indicate that the melt inclusions cooled rapidly. Second, post-entrapment crystallization of olivine averages less than 5% (Table 1) and no Fe–Mg zoning (indicating cation diffusion — see Danyushevsky et al., (2000) for further details) has been observed at inclusion rims, providing further evidence of rapid cooling after entrapment of the inclusions. Finally, there are no relationships between H_2O, δD and melt inclusion size, as would be expected from inclusions that had experienced hydrogen loss.

Hauri, (2002) showed experimentally that hydrogen loss from melt inclusions can occur when a diffusion gradient exists between the melt inclusion and the outside environment of the olivine. In his study, the melt inclusions were dehydrogenated by heating in an extremely dry 1-atm furnace, resulting in the maximum possible driving force for diffusion. Inclusion H_2O and D/H ratios are unaffected by 10 min of heating, but longer times can result in H_2O loss via proton diffusion and result in increases in D/H in the melt inclusions. For this reason, all samples analyzed in this study, with the exception of two inclusions from Anatahan volcano, were naturally glassy melt inclusions. Two Anatahan melt inclusions were reheated for 10 min; their volatile and D/H systematics are no different from the naturally glassy melt inclusions from the same sample.

4.2. H isotope exchange between inclusions and host magma

Hydrogen exchange between melt inclusions and host magma can also occur within magma reservoirs; for example, if the host crystals are mixed into a magma with a different water content. In this case, the diffusion gradients driving H exchange are likely to be even smaller than they are for post-eruptive diffusion, even though the time scales can be considerably longer. Our data set shows a negative correlation between H_2O and TiO_2 contents (Fig. 3), reflecting the well-established influence of H_2O on increasing the extent of melting of the sub-arc mantle (Kelley et al., 2006; Langmuir et al., 2006), and affirming that the water dissolved in our melt inclusions is magmatic water derived from the mantle source region of Mariana arc magmas.

If loss or exchange of water were significant and pervasive in our melt inclusions, correlations between H_2O and TiO_2 would not be preserved. Indeed, if hydrogen exchange attained equilibrium, we would expect homogeneous water contents (and D/H ratios) in the inclusions from individual hand samples (which are not observed). As a result, we consider hydrogen exchange between inclusions and surrounding magma to have been minor.

4.3. Estimating entrapment pressure of melt inclusions

Trapping pressures estimated for the Mariana melt inclusions using Dixon and Stolper's vapor saturation model (Dixon and Stolper, 1995) indicate that a majority of the inclusions were enclosed in their host crystals at depths of 3–15 km. The possibility that our melt inclusions assimilated meteoric water at such depths is unlikely. We find no relationship between δD and entrapment pressure, as would be expected if dry magmas assimilated meteoric water within Mariana volcanoes.

The CO_2 and H_2O contents of the melt inclusions (after bubble correction) can be used to calculate the pressure of vapor saturation (Psat; Table 1) (Dixon and Stolper, 1995). This pressure is regarded as a minimum pressure of melt inclusion entrapment, as it assumes that the magma trapped in the inclusion was in equilibrium with an exsolved vapor phase. The actual trapping pressure could be higher if the magma were undersaturated in a mixed CO_2–H_2O vapor.

The solubility of major volatile phases in a melt is strongly controlled by pressure and thus melt inclusions trapped at greater depth (i.e., higher Psat) could have undergone lower degrees of degassing and be more representative of the underlying mantle source. CO_2 and H_2O contents of Mariana arc melt inclusions span a wide range of values and do not fall along the simple open or closed-system degassing trends, based on projected degassing trends from our highest CO_2 concentration sample (Fig. 4). This indicates that (i) there may be some variability in the initial H_2O and CO_2 contents of individual batches of magma, and/or (ii) different amounts of gas may have been lost from different magma batches prior to melt inclusion entrapment.

4.4. Magmatic degassing

Based on studies of submarine glasses (Kyser and O'Neil, 1984) and melt inclusions from Hawaii (Hauri, 2002), as well as experimental hydrogen isotope fractionation studies (Pineau et al., 1998), degassing of H_2O from silicate melts can lead to low δD values and a positive correlation with H_2O contents when magma H_2O contents are <2 wt.%. There is no such correlation in our data set; instead, the full range of δD values is observed at both high (4 wt.%) and low (1.5 wt.%) H_2O contents (Fig. 2). This observation can be explained by the fact that a significant fraction of the water dissolved in our melt inclusions exists in the molecular form, rather than as OH, and the isotopic fractionation

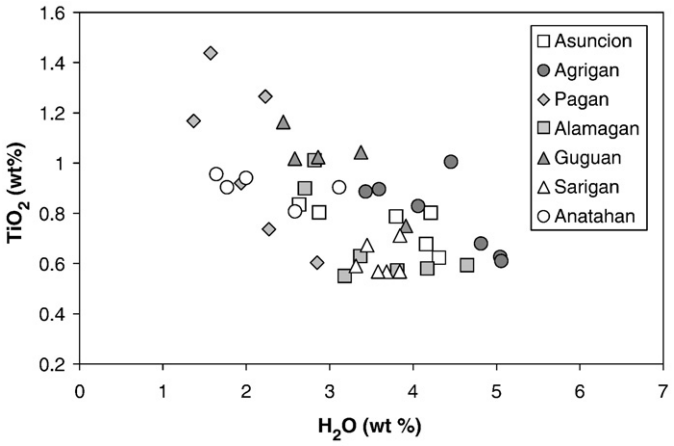

Fig. 3. The relationship between TiO_2 and H_2O. TiO_2 can be used as a proxy for the degree of melting (Kelley et al., 2006) and thus the observed negative relationship with H_2O reflects the influence of water on increasing the extent of melting in the sub-arc mantle.

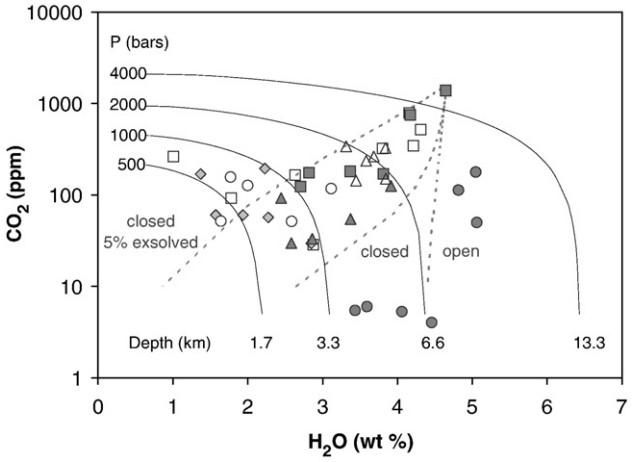

Fig. 4. CO_2 and H_2O contents of melt inclusions from the Mariana arc volcanoes — symbols are the same as in Fig. 2. The vapor saturation curves from Dixon and Stolper (1995) have been superimposed on the plot (solid curves) to show the pressure (or depth) of melt inclusion entrapment. We show closed- and open-system degassing trends (dashed lines; Dixon and Stolper, 1995) from an initial source having the composition of our highest CO_2 concentration sample (ALA-02_5). We also show the closed-system degassing trend for a melt with 5 wt.% exsolved vapor at its initial pressure.

expected between water vapor and dissolved molecular H_2O during magmatic degassing is close to zero (Newman et al., 1988). In contrast, most of the water dissolved in magmas with lower water concentrations exists as OH and fractionations between water vapor and dissolved OH can be significant (Newman et al., 1988). There is a positive correlation of CO_2 and H_2O contents in many of the Mariana melt inclusions, consistent with some volatile loss by degassing prior to melt inclusion entrapment; however, the expected shifts in δD with modest amounts of H_2O degassing are small. For example, even if 50% of the original water from sample ALA-02_5 was lost, the associated δD shift would be less than 8‰ (for a vapor–melt fractionation factor (α) of 1.012 — assuming that 50% of water would be bound as molecular water where α=1; Newman et al., 1988). It is clear from the volatile abundance relationships that degassing-related losses have occurred, but given that degassing-related δD shifts are relatively small compared with the observed δD range and that we find no relationship between water content and δD values (Fig. 2), we conclude that degassing is not the dominant process controlling δD values of Mariana arc melt inclusions.

Therefore, the water in our Mariana melt inclusions is magmatic water derived from the sub-arc mantle, little influenced by shallow-level processes. We cannot rule out some exchange between melt inclusions and host magma via diffusion through the olivine hosts, e.g., while the crystals resided in crustal magma reservoirs. However, the relationship between H_2O and TiO_2 in our data set (Fig. 3) is inherited from mantle melting, and indicates that hydrogen exchange was neither pervasive nor significant enough to alter the hydrogen isotope ratios of our melt inclusions. We note that there is no difference observed in δD of melt inclusions from Agrigan and Guguan volcanoes, the so-called sediment and altered oceanic crustal fluid endmembers. The high δD signatures of the melt inclusions are entirely consistent with the presence of a subduction component in the mantle wedge source of Mariana arc volcanoes.

5. Discussion

5.1. Alteration and dehydration of subducting lithosphere

The bulk hydrogen isotope composition of altered oceanic lithosphere reflects a mixture between magmatic mantle-derived water in mid-ocean ridge basalt (avg. δD −80±10‰, Kyser and O'Neil, 1984) and various hydrous minerals formed by hydrothermal alteration. The hydrogen isotope composition of a subducting slab is estimated at −50‰; this value is based on the average δD composition of hydrous mineral phases within the oceanic crust and serpentinized peridotite sections (Margaritz and Taylor, 1976; Agrinier et al., 1995). A compilation of equilibrium mineral–water D/H fractionations for common alteration minerals, determined experimentally over variable ranges of temperatures (100–1000 °C), are presented in Fig. 5 (Suzuoki and Epstein, 1976; Sakai and Tsutsumi, 1978; Lambert and Epstein, 1980; Graham et al., 1984; Vennemann and O'Neil, 1996; Saccocia et al., 2001). These fractionations predict the formation of seafloor alteration minerals with a wide range of δD values; however, a vast majority of the fractionations result in δD values similar to the hydrogen isotope composition of most authigenic marine sediments and seafloor serpentinites (−30±25‰; (France-Lanord and Sheppard, 1992; Lecuyer and O'Neil, 1994). It is the presence of variable amounts of these alteration minerals that elevates the bulk δD of altered seafloor by 10‰ to 30‰ above mantle values (Agrinier et al., 1995; Alt, 2003).

Several of the Mariana inclusions have δD values overlapping with the average slab value (−50‰), but the majority are significantly higher. If we compare our melt inclusion compositions to the bulk composition of the altered upper oceanic crustal value at site 801 (δD= −87‰ which we take to represent a lower limit for the subducting slab value (Alt, 2003), all of our samples are considerably higher. This indicates that slab dehydration has resulted in the release of water with D/H ratios that have been shifted to higher values. Although direct addition of seawater would result in elevated δD values, geochemical evidence does not support this. For example, we find no systematic increase in δD with increasing H_2O (Fig. 2) or Cl contents, as would be expected if direct seawater additions were significant. Chlorine contents are generally elevated in arc-derived melts due to slab additions, but in this case we find no relationship with δD, consistent with the notion that most non-chemically-bound seawater would be lost by compaction before reaching the zone of arc magma generation.

Based on values presented in Fig. 5, we suggest that the modern isotopic composition of the upper mantle (avg. δD −80‰) cannot simply reflect the steady-state subduction of seafloor alteration minerals (avg. δD −30‰), as first proposed by Taylor (1974) and re-emphasized by Javoy (2005). An additional fractionation of hydrogen isotopes is required to account for the 80‰ difference in δD between

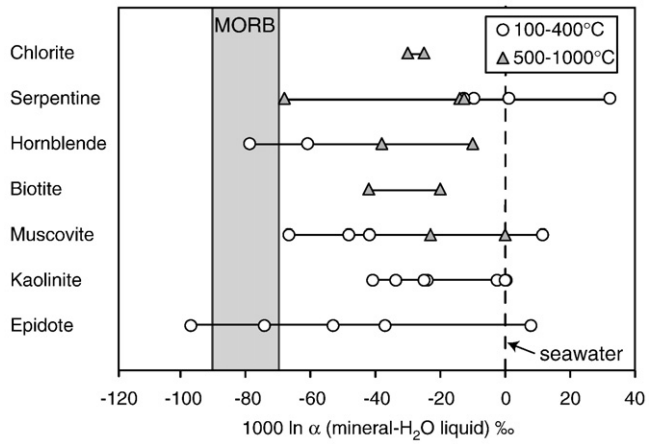

Fig. 5. Compilation of experimentally determined D/H fractionation factors (‰) between water and common alteration minerals (Suzuoki and Epstein, 1976; Sakai and Tsutsumi, 1978; Lambert and Epstein, 1980; Graham et al., 1984; Vennemann and O'Neil, 1996; Saccocia et al., 2001) as compared to the MORB range (shaded region). We have distinguished between values determined at relatively low temperatures (100–400 °C) versus higher temperatures (500–1000 °C). Because the δD of seawater is 0‰, these data also represent the δD values of these minerals in equilibrium with seawater. We note that the average ‰ fractionation between water and hydrous minerals is less than the 80‰ difference between MORB and seawater.

the oceans and the mantle. The elevated δD values of the Mariana melt inclusions relative to the upper mantle indicate that this fractionation takes place in subduction zones. A subducting lithospheric slab loses water more or less continuously as it proceeds along its subduction path (Schmidt and Poli, 1998) and hydrogen isotope fractionations associated with this dehydration provide an explanation for the δD values of our Mariana melt inclusions. Porewater within sediments, having δD essentially indistinguishable from seawater (0‰) down to values of −44‰ (France-Lanord and Sheppard, 1992), is mostly released to the oceans via compaction in the fore-arc region (Rüpke et al., 2002). Likewise, because clay minerals begin to dehydrate at ~250 °C and completely break down by ~450 °C, most of the chemically-bound water in marine sediments would likely be lost from the slab within the first 50 km of subduction (Schmidt and Poli, 1998; Rüpke et al., 2002). Various high-pressure mineral phases in the oceanic lithosphere then undergo metamorphic dehydration reactions as subduction proceeds, releasing water that induces melting beneath the arc. Chlorite, lawsonite, amphibole and serpentine likely contribute the bulk of the water that is released beneath magmatic arcs (Schmidt and Poli, 1998).

Experimentally determined fractionation factors between water and hydrous minerals indicate that the fluids released from the slab during dehydration should be enriched in deuterium (Suzuoki and Epstein, 1976; Sakai and Tsutsumi, 1978; Lambert and Epstein, 1980; Graham et al., 1984; Vennemann and O'Neil, 1996; Saccocia et al., 2001). If the isotopic composition of the subducting slab ranges from −50 to −87‰, then all of the variation observed in our melt inclusions can be explained by D/H fractionation during slab dehydration. Comparing the estimated average δD input value (−50‰) to the average melt inclusion output value (δD=−34±13‰; n=43), suggests that subduction-related fluids are enriched in D by +16‰ over altered MORB values, and by +46‰ over the mantle average.

5.2. Implications for deep-mantle water

The loss of a D-enriched fluid phase from the subducting slab has important consequences for any residual water that survives beyond the zone of magma generation beneath the arc. The fractionation of hydrogen isotopes during dehydration has the potential to create complementary D-enriched (mantle wedge) and D-depleted (slab) mantle components. Slab-bound water will evolve to progressively lower δD values as D-enriched water is released to the mantle wedge. Evidence of δD heterogeneity in the mantle comes from ocean island basalts (OIB). Exceptionally low δD values (to −165‰) have been measured in mantle xenoliths (Deloule et al., 1991) and melt inclusions (Hauri, 2002) from Koolau volcano in the Hawaiian Islands (see Fig. 2), the source of which is postulated to have a significant recycled slab component (Eiler et al., 1996; Hauri, 1996; Lassiter and Hauri, 1998). High δD values have been measured in glasses associated with the Salas y Gomez mantle plume, and have been ascribed to a D-rich recycled slab water signature (Kingsley et al., 2002); we suggest that this signature could be characteristic of recycled mantle wedge peridotite. A similar process has recently been postulated to explain Li isotope anomalies observed at the East Pacific Rise (Elliott et al., 2006). Given the paucity of H isotope studies in plume-related localities, the origin of OIB water is difficult to evaluate at this stage, but our findings support a process whereby subduction-related dehydration would result in D-depleted slabs and a D-enriched mantle wedge. Even with extensive slab dehydration (Dixon et al., 2002), both of these components would have H_2O contents higher than the upper mantle source of mid-ocean ridge basalts, and are available for convective transport into the deeper mantle.

A 2-reservoir mass-balance model can be used to describe the release of water from the subducting slab into the mantle wedge (Fig. 6). In this model, we consider dehydration of a slab with initial bulk δD values of −50‰ and −87‰ (where −87‰ would represent the case where the bulk of the water was released from the altered upper crustal section only). For a given D/H of fluid released to the mantle wedge, we can calculate the corresponding δD value of residual water in the subducting slab as dehydration progresses. For example, if the average δD value of Mariana melt inclusions (−34‰) is representative of the fluids released from the subducting slab, then a slab would need to lose 88% of its water to achieve a δD of −165‰ (a Koolau-like source). The resulting D/H shift of the slab is more than 100‰, a much larger isotopic effect than the 10‰ to 30‰ increase in δD resulting from seafloor alteration (Fig. 5). Based on the high water contents of Mariana arc melt inclusions, extents of slab dehydration are expected to be large. If slab dehydration is particularly efficient, as inferred from low H_2O/Ce ratios of plumes containing recycled lithosphere (Dixon et al., 2002), then the residual water in the subducting slab would become extremely D-depleted (e.g., δD=−234‰ for 92% water loss from a −50‰ slab).

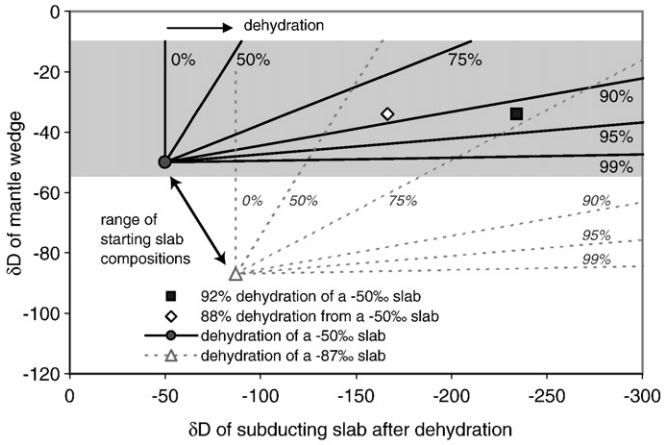

Fig. 6. The effect of dehydration on δD of the mantle wedge. The δD of fluids transferred to the mantle wedge depends on the starting slab composition, the extent of slab dehydration, and the δD value of the fluid residual in the slab. The solid and dashed lines show the extent of dehydration from a slab with initial δD compositions of −50‰ and −87‰, respectively; each line traces the δD value of the mantle wedge for a given δD value of the dehydrated slab. The shaded box shows the range of values measured in our Mariana melt inclusions. Taking the average δD of our melt inclusions (δD=−34‰) and assuming an initial slab composition of δD=−50‰, we show two examples: 1) a residual slab composition (−234‰) calculated assuming 92% dehydration (Dixon et al., 2002; filled square), and 2) the % dehydration required (88%) to produce a slab with a δD value of −165‰, as measured in Koolau melt inclusions (Hauri, 2002; open diamond).

5.3. Ocean–mantle exchange of H_2O

The amount of water that is ultimately transferred into the deep mantle via slabs is difficult to constrain, but generally considered to be relatively small (Dixon et al., 2002). However, given that the subduction process has likely been proceeding for at least 3 Ga (Witze, 2006), subduction-related D/H fractionation could have significantly modified the H isotope composition of Earth's reservoirs. In order to calculate how the isotopic composition of water in mantle and surface reservoirs has evolved over time, we examine mantle D/H variations in a 2-reservoir exchange model with hydrogen isotope fractionations associated with ocean crust alteration and slab dehydration. We assume: 1) the calculated bulk earth composition of water (based on δD and water contents of surface reservoirs (Lecuyer et al., 1998) and the mantle) is representative of water on Earth prior to the initiation of subduction, 2) the amount of water subducted to the mantle (beyond the zone of arc magma generation) is balanced by the amount of water added by hydrothermal alteration at ridges, 3) the D/H fractionations associated with dehydration (this study) and alteration of the slab (Margaritz and Taylor, 1976; Agrinier et al., 1995) can be constrained from the geochemical data; and 4) water input to the mantle is well

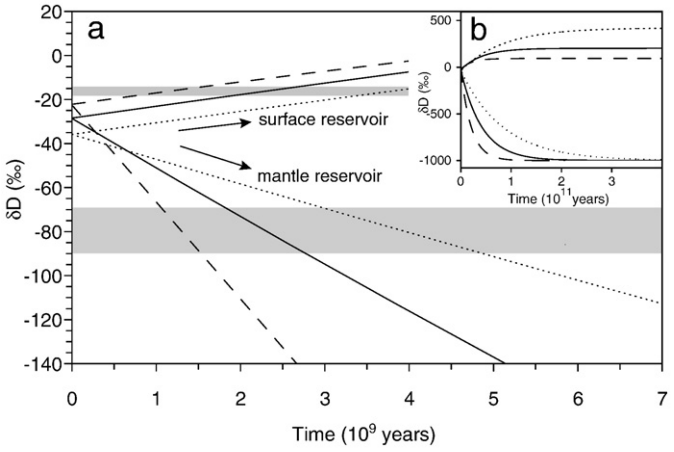

Fig. 7. a) A box model showing the evolution of H isotopes in Earth's surface and mantle reservoirs; the model includes the H_2O flux and D/H fractionations associated with ocean crust alteration and subduction dehydration — calculations outlined in Supplementary information. The net effect of these fractionations is a temporal increase in surface δD and decrease of mantle δD. We show evolution trends for 3 different cases: 1) a mantle with 100 ppm H_2O where the entire mantle convects (solid line), 2) a mantle with 100 ppm H_2O where only 50% of the mantle convects (dashed line), and 3) a mantle with 400 ppm H_2O where 50% of the mantle convects (dotted line). The gray fields represent the modern δD of the hydrosphere (upper field) and mantle (lower field), b) the same model showing the length of time required for the system to reach steady state for each of the different cases.

mixed over the time scales considered. This calculation is sensitive to the water content of the mantle, but mantle H_2O content is well constrained by studies of mid-ocean ridge and ocean island basalts (e.g., Michael, 1995; Danyushevsky et al., 2000; Dixon et al., 2002; Asimow et al., 2004). Likewise, the mass of the convecting mantle exchanging H_2O with the surface will influence the time required to produce the isotopic differences that we observe between surface and mantle reservoirs today.

In order to show the effect of the subduction process on H isotopes in mantle reservoirs, we consider three mantle convection scenarios into which an altered slab with 1% H_2O (water available at sub-arc depths) is introduced: (A) into a mantle with 100 ppm H_2O where the entire mantle convects, (B) into a mantle with 100 ppm H_2O where only 50% convects, and (C) into a wetter mantle with 400 ppm H_2O where only 50% of the mantle convects. Calculation details are outlined in the Supplementary materials. Fig. 7 shows isotopic evolution trends of the mantle and surface reservoirs for each of these cases. We find that D/H fractionation in subduction zones has an important effect on the isotopic composition of Earth's water reservoirs. In the first case, the δD composition of a mantle having relatively low water contents (100 ppm) would require ~2.3 Ga for the mantle and exosphere to acquire their present-day hydrogen isotope compositions. However, given geochemical constraints indicating that certain portions of the mantle have not been significantly mixed (e.g., primitive reservoirs with solar-like neon isotopes (Ballentine et al., 2005)) it is likely that only a fraction of the mantle is well mixed. If we consider a mantle where only 50% convects through the subduction zone — ridge system, significantly less time (1.3 Ga) is required to achieve present-day reservoir values (case 2). In contrast, significantly more time (3.9 Ga) would be required for the subduction process to modify the isotopic composition of a wetter mantle (=400 ppm H_2O). We note that by increasing the size of the mantle reservoir that is cycling through the subduction system, the time required to reach present-day δD values increases; likewise, increasing the water content of the mantle would produce a similar increase in requisite time. Most importantly, the D-enrichment in altered MORB, and the larger D-enrichment of subduction zone water contained in our Mariana melt inclusions, shows that there exists today a net flux of deuterium (relative to hydrogen) out of the mantle and into the exosphere. The corresponding net D-depletion of the mantle shows that the surface-mantle exchange of hydrogen isotopes is not presently at steady state, consistent with our exchange model.

6. Conclusions

It is clear that the subduction process has a considerable effect on the isotopic composition of Earth's water reservoirs. The elevated δD values of our Mariana melt inclusions (−55 to −12‰) show that subduction releases a D-enriched fluid to the source region of arc magmas. The corollary of this observation is that a D-depleted slab must be subducted to the deeper mantle. This model is illustrated in Fig. 8 and predicts that OIBs with recycled slab components should have low δD values, while OIBs containing recycled mantle wedge material should exhibit high δD values. This conclusion is robust irrespective of the mantle's water content or the degree to which the slab dehydrates. Our findings also suggest that subduction dehydration is the dominant process controlling D/H ratios in the deep-Earth water cycle, and is thus responsible for the difference in δD between mantle and surface water that is observed today.

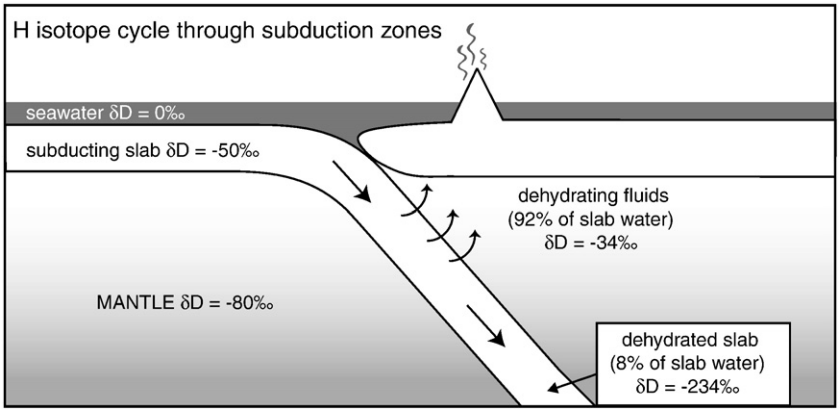

Fig. 8. Schematic diagram showing our proposed model for how H isotopes in Earth's reservoirs are cycled through the subduction zone system. We illustrate the effect of the dehydration process on H isotopes using the example discussed in the text — 92% dehydration of the slab with the fluids released having an average δD of −34‰. An important consequence of this process is that the down-going slab would have extremely low δD values and thus we predict that OIBs with significant recycled slab components would also have low δD values. In contrast, OIBs with a dehydration-related subduction fluid component would have high δD values.

Acknowledgements

This work was generously supported by grants from the NSF MARGINS program: OCE-0305218 (Fischer), OCE-0305248 (Hilton), OCE-0305052 (Hauri). Fieldwork on the remote Mariana Islands would not have been possible without the assistance of various people including Patrick Shore and Doug Wiens (Washington University), Mike Cunningham (Americopters), the Emergency Management Office in Saipan, and the crews of the Super Emerald and the R/V Wecoma. We thank Chris Hadidiacos (Geophysical Laboratories) for technical assistance with electron microprobe measurements. We would especially like to thank Jianhua Wang (DTM) for his expert knowledge of and assistance with Carnegie's ion microprobe.

Appendix A. Supplementary data

Supplementary data associated with this article can be found, in the online version, at doi:10.1016/j.epsl.2008.08.015.

References

Agrinier, P., Hékinian, R., Bideau, D., Javoy, M., 1995. O and H stable isotope compositions of oceanic crust and upper mantle rocks exposed in the Hess Deep near the Galapagos Triple Junction. Earth Planet. Sci. Lett. 136, 183–196.

Allard, P., 1983. The origin of hydrogen, carbon, sulphur, nitrogen and rare gases in volcanic exhalations; evidence from isotope geochemistry. In: Tazieff, H., Sabroux, J.-C. (Eds.), Forecasting Volcanic Events. Elsevier, Amsterdam, pp. 337–386.

Alt, J.C., 2003. Stable isotopic composition of upper oceanic crust formed at a fast spreading ridge, ODP Site 801. Geochem. Geophys. Geosys. 4. doi:10.1029/2002GC000400.

Asimow, P.D., Dixon, J.E., Langmuir, C.H., 2004. A hydrous melting and fractionation model for mid-ocean ridge basalts: application to the Mid-Atlantic Ridge near the Azores. Geochem. Geophys. Geosyst. 5. doi:10.1029/2003GC000568.

Ballentine, C.J., Marty, B., Sherwood Lollar, B., Cassidy, M., 2005. Neon isotopes constrain convection and volatile origin in the Earth's mantle. Nature 433, 33–38.

Danyushevsky, L.V., Eggins, S.M., Falloon, T.J., Christie, D.M., 2000. H2O abundance in depleted to moderately enriched mid-ocean ridge magmas; Part I: incompatible behavior, implications for mantle storage, and origin of regional variations. J. Petrol. 41, 1329–1364.

Deloule, E., Albarede, F., Sheppard, M.F., 1991. Hydrogen isotope heterogeneities in the mantle from ion probe analysis of amphiboles from ultramafic rocks. Earth Planet. Sci. Lett. 105, 543–553.

Dixon, J.E., Stolper, E.M., 1995. An experimental study of water and carbon dioxide solubilities in mid ocean ridge basaltic liquids. Part II: applications to degassing. J. Petrol. 36, 1633–1646.

Dixon, J.E., Leist, L., Langmuir, C.H., Schilling, J.G., 2002. Recycled dehydrated lithosphere observed in plume-influenced mid-ocean ridge basalt. Nature 420, 385–389.

Eiler, J.M., Farley, K.A., Valley, J.W., Hofmann, A.W., Stolper, E.M., 1996. Oxygen isotope constraints on the sources of Hawaiian volcanism. Earth Planet. Sci. Lett. 144, 453–468.

Elliott, T., Plank, T., Zindler, A., White, W., Bourdon, B., 1997. Element transport from slab to volcanic front at the Mariana arc. J. Geophys. Res. 102, 14991–15019.

Elliott, T., Thomas, A., Jeffcoate, A., Niu, Y.L., 2006. Lithium isotope evidence for subduction-enriched mantle in the source of mid-ocean-ridge basalts. Nature 443, 565–568.

France-Lanord, C., Sheppard, S.M.F., 1992. Hydrogen isotope composition of pore waters and interlayer water in sediments from the central western Pacific, Leg 129. Proc. Ocean Drill. Program Sci. Results 129, 295–302.

Galer, S.J.G., 1991. Interrelationships between continental freeboard, tectonics and mantle temperature. Earth Planet. Sci. Lett. 105, 214–228.

Giggenbach, W.F., 1992. Isotopic shifts in waters from geothermal and volcanic systems along convergent plate boundaries and their origin. Earth Planet. Sci. Lett. 113, 495–510.

Graham, C.M., Harmon, R.S., Sheppard, S.M.F., 1984. Experimental hydrogen isotope studies: hydrogen isotope exchange between amphibole and water. Am. Mineral. 69, 128–138.

Hauri, E.H., 1996. Major-element variability in the Hawaiian mantle plume. Nature 382, 415–419.

Hauri, E., 2002. SIMS analysis of volatiles in silicate glasses, 2: isotopes and abundances in Hawaiian melt inclusions. Chem. Geol. 183, 115–141.

Hauri, E., et al., 2002. SIMS analysis of volatiles in silicate glasses 1. Calibration, matrix effects and comparisons with FTIR. Chem. Geol. 183, 99–114.

Hauri, E.H., et al., 2006. Matrix effects in hydrogen isotope analysis of silicate glasses by SIMS. Chem. Geol. 235, 352–365.

Ishikawa, T., Tera, F., 1999. Two isotopically distinct fluid components involved in the mariana arc: evidence from Nb/B ratios and B, Sr, Nd, and Pb isotope systematics. Geology 27, 83–86.

Jambon, A., Zimmermann, J.L., 1990. Water in oceanic basalts — evidence for dehydration of recycled crust. Earth Planet. Sci. Lett. 101, 323–331.

Javoy, M., 2005. Where do the oceans come from? C. R. Geoscience 337, 139–158.

Kelley, K.A., et al., 2006. Mantle melting as a function of water content beneath back-arc basins. J. Geophys. Res. 111. doi:10.1029/2005JB003732.

Kent, A.J.R., Elliott, T.R., 2002. Melt inclusions from Marianas Arc lavas; implications for the composition and formation of island arc magmas. Chem. Geol. 183, 263–286.

Kingsley, R.H., et al., 2002. D/H ratios in basalt glasses from the Salas y Gomez mantle plume interacting with the East Pacific Rise: water from old D-rich recycled crust or primordial water from the lower mantle? Geochem. Geophys. Geosyst. 3, U23–U48.

Kyser, T.K., O'Neil, J.R., 1984. Hydrogen isotope systematics of submarine basalts. Geochim. Cosmochim. Acta 48, 2123–2133.

Lambert, S., Epstein, S., 1980. Stable isotope investigations of an active geothermal system in Valles Caldera, Jemez Mountains, New Mexico. J. Volcanol. Geotherm. Res. 9, 111–129.

Langmuir, C.H., Bezos, A., Escrig, S., Parman, S.W., 2006. Chemical systematics and hydrous melting of the mantle in back-arc basins. In: Christie, D., Fisher, C. (Eds.), Back Arc Spreading Systems—Geological, Biological, Chemical and Physical Interactions. AGU Geophysical Monograph, vol. 166, pp. 87–146.

Lassiter, J.C., Hauri, E.H., 1998. Osmium-isotope variations in Hawaiian lavas; evidence for recycled oceanic lithosphere in the Hawaiian Plume. Earth Planet. Sci. Lett. 164, 483–496.

Lecuyer, C., O'Neil, J.R., 1994. Stable isotope compositions of fluid inclusions in biogenic carbonates. Geochim. Cosmochim. Acta 58, 353–363.

Lecuyer, C., Gillet, P., Robert, F., 1998. The hydrogen isotope composition of seawater and the global water cycle. Chem. Geol. 145, 249–261.

Margaritz, M., Taylor, H.P., 1976. Oxygen, hydrogen and carbon isotopes studies of Franciscan Formation, Coast Range, California. Geochim. Cosmochim. Acta 40, 215–237.

Michael, P., 1995. Regionally distinctive sources of depleted MORB: evidence from trace elements and H2O. Earth Planet. Sci. Lett. 131, 301–320.

Miyagi, I., Matsubaya, O., 2003. Hydrogen isotopic composition of hornblende and biotite phenocrysts from Japanese Island arc volcanoes; evaluation of alteration process of the hydrogen isotopic ratios by degassing and re-equilibration. J. Volcanol. Geotherm. Res. 126, 157–168.

Newman, S., Epstein, S., Stolper, E., 1988. Water, carbon-dioxide, and hydrogen isotopes in glasses from the ca 1340 A.D. Eruption of the Mono Craters, California — constraints on degassing phenomena and initial volatile content. J. Volcanol. Geotherm. Res. 35, 75–96.

Newman, S., Stolper, E., Stern, R., 2000. H_2O and CO_2 in magmas from the Mariana arc and back arc systems. Geochem. Geophys. Geosyst. 1 1999GC000027.

Pineau, F., Shilobreeva, S., Kadik, A., Javoy, M., 1998. Water solubility and D/H fractionation in the system basaltic andesite–H_2O at 1250 °C and between 0.5 and 3 kbars. Chem. Geol. 147, 173–184.

Poreda, R., 1985. Helium -3 and deuterium in back-arc basalts; Lau Basin and the Mariana Trough. Earth Planet. Sci. Lett. 73, 244–254.

Rupke, L.H., Phipps Morgan, J., Hort, M., Connolly, J.A.D., 2004. Serpentine and the subduction zone water cycle. Earth Planet. Sci. Lett. 223, 17–34.

Rüpke, L.H., Phipps Morgan, J., Hort, M., Connolly, J.A.D., 2002. Are the variations in Central American arc lavas due to differing basaltic versus peridotitic slab sources of fluids? Geology 30, 1035–1038.

Saccocia, P.J., Seewald, J.S., Shanks, W.C., 2001. New D–H and 18O–16O fractionation factors for serpentine and talc from 250 to 450 °C. EOS Trans. AGU V51B–0991.

Sakai, H., Tsutsumi, M., 1978. D/H fractionation factors between serpentine and water at 100° to 500 °C and 2000 bar water pressure, and the D/H ratios of natural serpentines. Earth Planet. Sci. Lett. 40, 231–242.

Schmidt, M.W., Poli, S., 1998. Experimentally based water budgets for dehydrating slabs and consequences for arc magma generation. Earth Planet. Sci. Lett. 163, 361–379.

Stern, R.J., Fouch, M.J., Klemperer, S., 2003. An overview of the Izu–Bonin–Mariana subduction factory. In: Eiler, J. (Ed.), Inside the Subduction Factory. AGU Monograph, Washington DC, pp. 175–222.

Stolper, E., Newman, S., 1994. The role of water in the petrogenesis of Mariana Trough magmas. Earth Planet. Sci. Lett. 121, 293–325.

Suzuoki, T., Epstein, S., 1976. Hydrogen isotope fractionation between OH-bearing minerals and water. Geochim. Cosmochim. Acta 40, 1229–1240.

Taran, Y.A., Pokrovsky, B.G., Esikov, A.D., 1989. Deuterium and oxygen-18 in fumarolic steam and amphiboles from some Kamchatka volcanoes: 'andesitic waters'. Dokl. Akad. Nauk, USSR 304, 440–443.

Taylor, H.P., 1974. The application of oxygen and hydrogen isotope studies to problems of hydrothermal alteration and ore deposition. Econ. Geol. 69 843-843.

Tollstrup, D.L., Gill, J.B., 2005. Hafnium systematics of the Mariana arc: evidence for sediment melt and residual phases. Geology 33, 737–740.

Vennemann, T.W., O'Neil, J.R., 1996. Hydrogen isotope exchange reactions between hydrous minerals and molecular hydrogen: I. A new approach for the determination of hydrogen isotope fractionation at moderate temperatures. Geochim. Cosmochim. Acta 60, 2437–2451.

Walker, J.A., Roggensack, K., Patino, L.C., Cameron, B.I., Matias, O., 2003. The water and trace element contents of melt inclusions across an active subduction zone. Contrib. Mineral. Petrol. 146, 62–77.

Witze, 2006. The start of the world as we know it. Nature 442, 128–131.